ARTICLE

Check for updates

Probe for bound states of SU(3) fermions and colour deconfinement

Wayne J. Chetcuti [1,2,3✉], Juan Polo[3], Andreas Osterloh [3], Paolo Castorina[2,4] & Luigi Amico[2,3,5,6]

Fermionic artificial matter realized with cold atoms grants access to an unprecedented degree of control on sophisticated many-body effects with an enhanced flexibility of the operating conditions. Here, we consider three-component fermions with attractive interactions to study the formation of complex bound states, whose nature goes beyond the standard fermion pairing occurring in quantum materials. Such systems display clear analogies with quark matter. We address the nature of the bound states of a three-component fermionic system in a ring-shaped trap through the persistent current. In this way, we demonstrate that we can distinguish between color superfluid and trionic bound states. By analyzing finite temperature effects, we show how finite temperature can lead to the deconfinement of bound states. For weak interactions, the deconfinement occurs because of scattering states. In this regime, the deconfinement depends on the trade-off between interactions and thermal fluctuations. For strong interactions the features of the persistent current result from the properties of a suitable gas of bound states.

[1] Dipartimento di Fisica e Astronomia "Ettore Majorana", Via S. Sofia 64, 95127 Catania, Italy. [2] INFN-Sezione di Catania, Via S. Sofia 64, 95127 Catania, Italy. [3] Quantum Research Center, Technology Innovation Institute, P.O. Box 9639 Abu Dhabi, UAE. [4] Institute of Particle and Nuclear Physics, Charles University, Prague, Czech Republic. [5] Centre for Quantum Technologies, National University of Singapore, 3 Science Drive 2, Singapore 117543, Singapore. [6] LANEF 'Chaire d'excellence', Université Grenoble-Alpes & CNRS, F-38000 Grenoble, France. ✉email: wayne.chetcuti@dfa.unict.it

Mutually attracting quantum many-body systems can form bound states. Their nature depends on the particles' quantum statistics. Bosons can give rise to 'bright solitons' in which all the particles are bound together[1–4]. Due to the Pauli exclusion principle, such states are hindered for fermions. Nevertheless, two-component fermions with opposite spin can form bounded pairs[5].

The advent of ultracold atomic systems has enabled the investigation of many-body systems made of interacting N-component fermions in the laboratory: the so-called SU(N) fermions[6–11]. In contrast to their two-component counterparts, N-component fermions can form bound states of different type and nature. Here, we focus on SU(3) fermions. On one hand, this can provide paradigmatic features of the bound states that can be formed for the general cases of $N > 2$. On the other, three-component fermions are of special interest because of their potential to mimic quarks and specific aspects of quantum chromodynamics (QCD)[12–15] for which it is clearly advantageous to explore "low-energy" quantum analogues[16–20]. Specifically, SU(3) fermions can form two types of bound states: a colour superfluid (CSF) wherein two colours are paired, and the other is unpaired; and a trion where all colours are involved in the bound state. Trions and CSFs are the analogues of hadrons and quark pairs in QCD. As such, important aspects of the QCD phase diagram like colour deconfinement and resonance formation in nuclear matter, can be analysed in cold atom platforms.

Fuelled by the recent aforementioned research activity in quantum technology, a considerable interest has been devoted to three-component fermions[13–15,21–27]. However, devising physical observables paving the way to explore the nature of the SU(3) bound states in cold atoms systems remains a challenging problem.

In this paper, we demonstrate how the frequency of the persistent current in a ring-shaped gas of three-component fermions pierced by an effective magnetic field, can provide the sought-after observable to study the problem. The persistent current is a matter-wave current probing the phase coherence of the system[28], that in line with the recent research activity in atomtronics[29,30], can be exploited as a diagnostic tool to explore quantum states. Persistent currents have been observed experimentally for both bosonic[31–34] and very recently fermionic systems[35,36].

Very important for our approach is the Leggett theorem, stating that the persistent current periodicity is dictated by the system's effective flux quantum[37]. For example, the effective flux quantum of a gas of non-interacting particles is the bare flux ϕ_0; while in a gas of Cooper pairs, the period is halved since a flux quantum is shared by two particles[38,39]. A persistent current with a periodicity reduced by the total number of particles $1/N_p$ has been found, indicating the formation of an N_p-bound state in bosonic systems[40–42]. Recently, the persistent current was used to investigate an SU(N) fermionic atomtronic circuit with repulsive interactions[43,44].

In our work, trion and CSF bound states correspond to specific ways in which the persistent current responds to the effective magnetic field. By monitoring the persistent current for different interaction regimes, we demonstrate how thermal fluctuations can lead to a specific deconfinement of the bound states. As an experimental probe in the cold atoms quantum technology, we analyse the time-of-flight imaging[29,30,32,45,46].

Results

Setup. To model N_p strongly interacting three-colour (component/species) fermions trapped in an L-site ring-shaped lattice pierced by an effective magnetic flux ϕ, we employ the SU(3) Hubbard model

$$\mathcal{H} = \sum_{j=1}^{L} \sum_{\alpha=1}^{3} \left[-t(e^{i\frac{2\pi\phi}{L}} c_{j,\alpha}^\dagger c_{j+1,\alpha} + \text{h.c.}) + \sum_{\beta > \alpha} U_{\alpha\beta} n_{j,\alpha} n_{j,\beta} \right] \quad (1)$$

where $c_{j,\alpha}^\dagger$ creates a fermion with colour α on site j, and $n_{j,\alpha} = c_{j,\alpha}^\dagger c_{j,\alpha}$ is the local particle number operator. The parameters t and $U_{\alpha\beta}$ denote the hopping amplitude and interaction strength respectively. We consider attractive interactions i.e. $U_{\alpha\beta} < 0$ and $t = 1$ fixes the energy scale. The effective magnetic field is realized through Peierls' substitution $t \to te^{i\frac{2\pi\phi}{L}}$.

In the continuous limit of vanishing lattice spacing or, equivalently, the dilute lattice limit $\nu = N_p/L \ll 1$ the physics of the system can be captured by the Gaudin–Yang–Sutherland model[47,48]. According to the general Bethe Ansatz machinery, the energy of the system is obtained after a set of coupled non-linear equations—the Bethe equations—are solved for the quasimomenta k_j of the system. The spectrum is obtained by such k_j, and results to be labelled by a specific set of quantum numbers[47,49] (see Supplementary Note 1). Bound states result from complex values of the quasimomenta (see Supplementary Note 2). In the limit of large $UL/t \gg 1$, the spectrum of the SU(3) Gaudin–Yang–Sutherland regime of the Hubbard model is obtained by solving a set of three equations, the so-called Takahashi equations, parametrized by n_1, n_2 and n_3 denoting the number of unpaired, pairs, and trions respectively (see Supplementary Note 2). We point out that the strongly attractive regime of model (1) cannot be recast into a Lai–Sutherland antiferromagnet since the condition of one particle per site cannot be achieved[10,50]. Bound states of different nature can arise in systems described by model (1): CSF bound states, wherein two colours form a bound pair with the other colour remaining unpaired; trions, wherein all the three colours form a bound state. CSF bound states can be achieved by breaking the SU(3) symmetry[15,22,24,25,27]. Here, we break the SU(3) symmetry explicitly in the canonical ensemble by choosing asymmetric interactions between the different colours (see[24,25,27] for symmetry breaking in the grand-canonical ensemble by adjusting the chemical potentials for each species). In the following, U refers to symmetric interactions between all colours.

SU(3) bound states of model (1) have been recently studied through correlation functions due to their relevance in emulating quark matter[15,23,26]. It is important to stress such systems are only analogues as they lack key features of quark matter such as string breaking and colour charge screening. The probe we use to study the system is the persistent current $I(\phi)$, which is the response to the effective magnetic flux threading the system: $I(\phi) = -\partial F(\phi)/\partial \phi$, with F being the system's free energy in the canonical ensemble[38]. The zero temperature persistent current arises only from the ground-state energy E_0, such that $I(\phi) = -\partial E_0(\phi)/\partial \phi$. Relying on the experimental capability of addressing fermions of different colours separately[11], especially to analyse the broken SU(3) cases, we utilize the species-wise persistent current: $I_\alpha = -\partial F_\alpha(\phi)/\partial \phi$. We point out that this calculation cannot be easily implemented in Bethe ansatz. The reason being that the species-wise persistent current has to be done with two-point correlations, which is very challenging in Bethe ansatz.

An important result in the field, due to Leggett, states that the energy of a many-body system displays periodic oscillations with the flux ϕ[37]. If single particle states are involved in the persistent current, the period is the bare one $\phi_0 = \hbar/mR^2$, with m and R denoting the atoms' mass and ring radius, respectively. When bound states are formed, the corresponding effective mass leads to a reduced periodicity in ϕ_0[38,40,51].

In cold atom systems, it has been demonstrated that most features of $I(\phi)$ can be observed through time-of-flight (TOF)

imaging[52]. TOF expansion entails the calculation of the particle density pattern $n_\alpha(\mathbf{k}) = |w(\mathbf{k})|^2 \sum_{j,l} e^{i\mathbf{k}\cdot(\mathbf{x}_j - \mathbf{x}_l)} \langle c_{j,\alpha}^\dagger c_{l,\alpha} \rangle$ where $w(\mathbf{k})$ are the Fourier transforms of the Wannier function and $\mathbf{x}_j$ denotes the position of the lattice sites in the plane of the ring. From the experimental side, $n(\mathbf{k})$ can be accessed through contrast image measurement of the density distribution after a TOF expansion of the condensate is carried out by switching off the confinement potential[30,52]. The variance of the width of the momentum distribution is given by $\sigma_{n_k}^{(\alpha)} = \sqrt{\langle \hat{n}_\alpha^2 \rangle - \langle \hat{n}_\alpha \rangle^2}$.

Zero temperature persistent current of SU(3) bound states. For small U, $I(\phi)$ is found to be a function with a period of the bare flux quantum ϕ_0. However, for stronger U, $I(\phi)$ displays fractionalization reducing its period. In contrast to attracting bosons[4,40,42] or repulsing N-component fermions[43,53], for attracting N-components fermions with symmetric interactions, the reduction of the period is dictated by N irrespective of N_p. In the SU(3) symmetric case, we find that trions are formed for arbitrary small attraction (see works[10,26]) in the three particle sector. This is corroborated by exact results based on the Bethe Ansatz analysis of the Gaudin-Yang Sutherland model (see Supplementary Note 3) and by the analysis of three-body correlation functions. In this regime and large UL/t, the analysis based on Takahashi's equations, demonstrates a perfect tri-partition of the period $\phi_0/3$ that amounts to the formation of a three-body bound state (Fig. 1b). By Bethe ansatz analysis, we find the exact expression of the zero temperature $I(\phi)$ in the continuous limit for a system consisting solely of trions in the limit of large U:

$$I(\phi) = -6\left(\frac{2\pi}{L}\right)^2 \left[\frac{K_a}{3} + \phi\right] \quad (2)$$

where K_a denotes the aforementioned quantum numbers. This implies that as the flux is increased, K_a need to shift to counteract this increase in flux (see Supplementary Note 2). Here, level crossings occur between the ground and excited states, causing the fractionalization. Discrete excitations can only partially compensate for the increase in flux, causing oscillations with a reduced period of $1/N$, thereby accounting for the 'size' of the bound state. For the CSF, which is out of reach of Bethe ansatz due to SU(3)-symmetry breaking, $I(\phi)$ displays a halved periodicity $\phi_0/2$ for the paired colours and a bare periodicity ϕ_0 for the unpaired colour (Fig. 1a). Further confirmation on the nature of the bound states is achieved through the analysis of correlation functions (see Supplementary Note 4).

It is worthwhile to point out that there are several routes in which a trion can be created in our system depending on if the system is endowed with isotropic interactions or anisotropic ones (see Supplementary Note 5). Additionally, the specific parity

effects of the persistent current are observed to not be washed out upon fractionalization contrary to the repulsive and attractive two-component cases (see Supplementary Note 6).

Finite temperature effects and colour deconfinement. The interplay between temperature T and attractive interaction U leads to peculiar effects in the persistent current $I(\phi)$: Besides the generic smoothening of the saw-tooth behaviour, finite temperature leads to specific changes in the frequencies of $I(\phi)$ depending on the interaction –Fig. 2. Such a phenomenon is consistent with the thermal effects on two-component fermions with repulsive interactions[54], which we show also holds for attractive interactions, irrespective of the number of particles in the system (see Supplementary Note 7). In the following, we discuss the thermal effects on the SU(3) symmetric interaction case (finite temperature CSF case is discussed in Supplementary Note 7). For small and moderate interactions, the analysis shows that $I(\phi)$, and its frequency in particular, arise from thermal fluctuations populating the scattering states (for the band structure of the system see the work[26] and Supplementary Note 7). Here, the relevant parameter is the relative size between interaction U and thermal fluctuations T (measured in units of t/k_B). At moderate U the bound states can remain well-defined for large U/T, whilst for smaller values of U/T the bound states' deconfinement occurs because the temperature makes scattering states accessible. On increasing U, the relevant contributions to $I(\phi)$ come from the bound states' sub-band only. For such a 'gas of bound states', the periodicity of $I(\phi)$ changes because the temperature allows the different frequencies of the excited states to contribute to the current. In this regime, since the level spacing between the bound states energy levels decreases, the thermal effects are increasingly relevant by increasing U.

To study the specific dependence of $I(\phi)$ on T and U, we analyse its power spectrum. Specifically, we consider the Fourier weight C_3 of $I(\phi)$ corresponding to trion formation at different U values and follow its decay with increasing temperature (see Supplementary Note 7 for the explicit definition). Such a weight corresponds to the reduced tri-partite periodicity corresponding to the formation of trions. This coefficient is rescaled by the maximum amplitude $|I_{max}|$ of $I(\phi)$. We find that $C_3/|I_{max}| = U^{-\lambda} G(T - T^*)$, in which λ, T^* (see Fig. 3 caption) and the function G as shown in Fig. 3a, c are markedly distinct in the aforementioned different interaction regimes (see also Supplementary Note 7). In the cross-over region between the colour deconfinement region and the bound states gas, the two regimes result to be indistinguishable (Fig. 3b).

Time of flight. Persistent currents can be probed in cold atom systems through TOF. To read out the nature of the states in our system, it is necessary that such images arise as an interference pattern of the gas wave functions. For the specific case of coherent neutral matter circulating with a given angular momentum, a
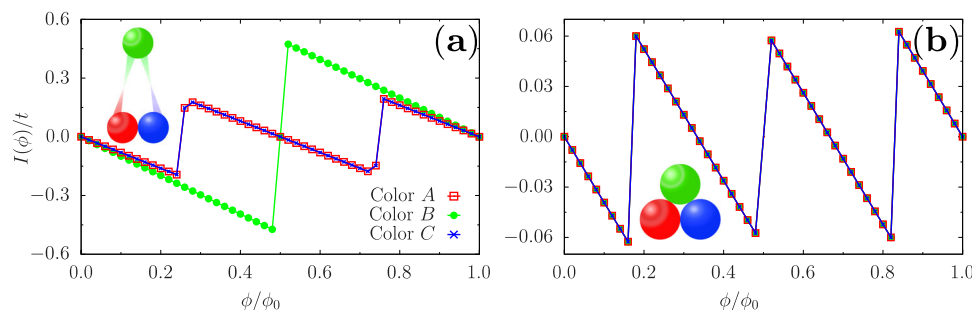
Fig. 1 Persistent currents of colour superfluids (CSFs) and trions. Persistent current $I(\phi)$ of the three colours (red squares, green circles, blue crosses) against the effective magnetic flux ϕ/ϕ_0. **a**, **b** depict the persistent current of a CSF and trion respectively. The interactions for the CSF are $|U_{AB}|/t = |U_{BC}|/t = 0.01$ and $|U_{AC}|/t = 3$. For a trion, $|U|/t = 3$ for all colours. All presented results are obtained for $N_p = 9$, $L = 15$ and using DMRG. The lines are meant to be a guide to the eye for the reader, to aid in perceiving the fractionalization.
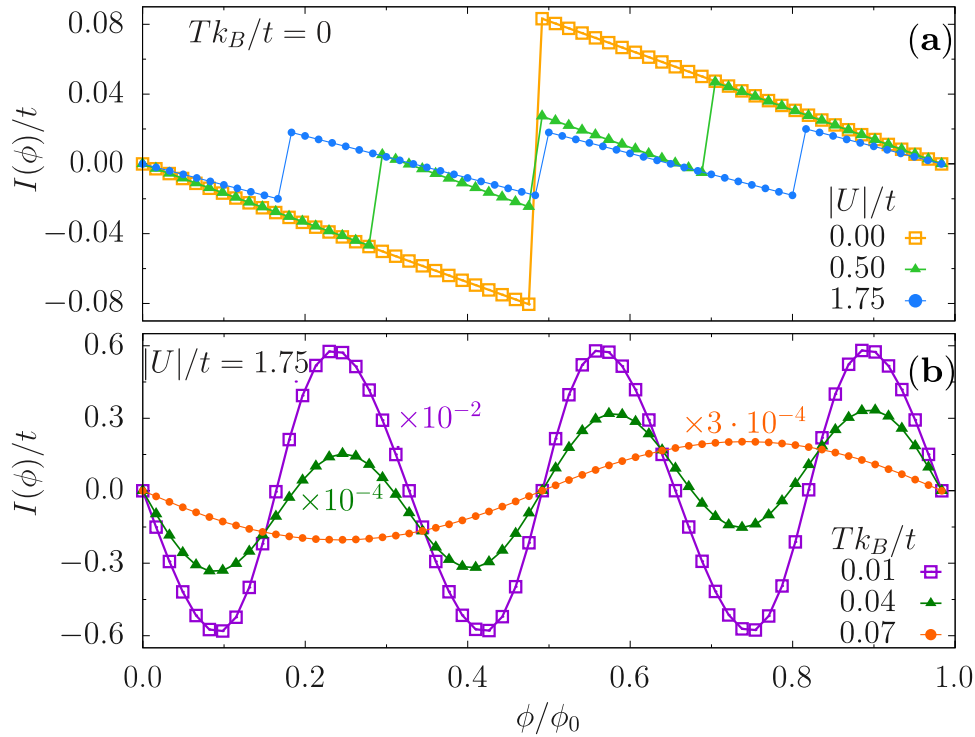
Fig. 2 Persistent current dependence on the interplay between temperature and interaction. Persistent current $I(\phi)/t$ of SU(3) fermions for various interactions U/t (temperatures Tk_B/t) in the upper (lower) panel. In **a** for $Tk_B/t = 0$, the persistent current fractionalizes with increasing U/t. The bare period ϕ_0/t is reduced to ϕ_0/N for large U/t. For fixed U/t in **b**, the persistent current regains the period ϕ_0 upon increasing Tk_B/t. The results were obtained by exact diagonalization with $N_p = 3, L = 15$. The lines are meant to be a guide to the eye for the reader, to aid in perceiving the fractionalization with increasing interaction.
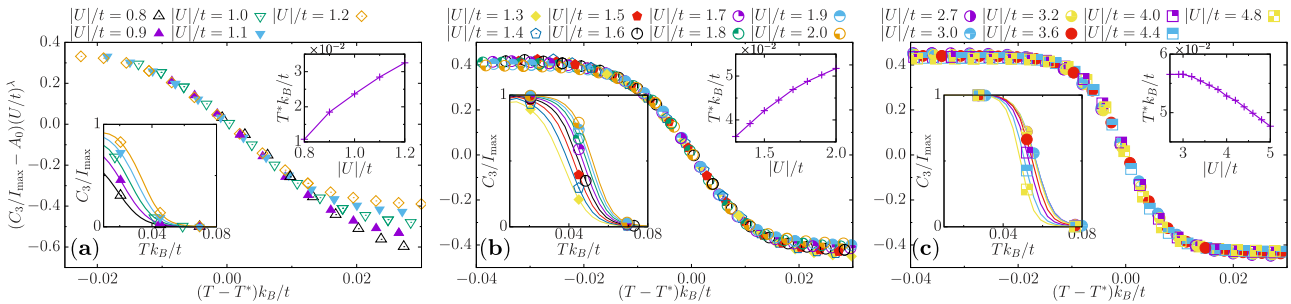

Fig. 3 Quantitative analysis of the persistent current scaling as a function of temperature and interaction. Interplay between temperature Tk_B/t and interaction U/t for the persistent current $I(\phi)/t$, by monitoring the Fourier weight C_3/t of the current that reflects its tri-partite periodicity. This coefficient decreases upon increasing temperature showing the breakdown of trions and in turn deconfinement. The three plots demonstrate that $C_3(T^*)/I_{max}(T^*)$ obeys distinct laws in the different regimes of interaction discussed in the text, where I_{max}/t is the maximum persistent current used to re-scale the Fourier weight across different interactions. The constant shift in $C_3(T^*)/I_{max}(T^*)$, is fixed for all curves by $A_0 = 0.5$. Top right insets display the temperature displacement T^*k_B/t as a function of U/t. Lower left insets show the raw data as a function of Tk_B/t. T^*k_B/t is defined by $C_3(T^*)/I_{max}(T^*) = 1/2$. In the regime of weak U/t displayed in **a**, $\lambda = -1.25$ and T^*k_B/t is an increasing function of $|U|/t$. For intermediate U/t depicted in **b**, $\lambda = -0.33$ and T^*k_B/t is still increasing, but with a different algebraic law. For the strong U/t regime in **c**, $\lambda = -0.1$ and T^*k_B/t is decreasing with $|U|/t$. All results were obtained with exact diagonalization for $N_p = 3, L = 15$ with the temperature Tk_B/t ranging from 0.01 to 0.08. Note that in the lower left insets only a few data points are displayed to enhance the readability of the figure.

characteristic hole is displayed. Due to the reduced coherence, no holes have been found in TOF for bound states (see exponential decay of correlations in the Supplementary Note 4)[41,51,55,56]. Nevertheless, current states and the corresponding angular momentum quantization emerge in the variance σ of the width of the momentum distribution as discrete steps. Here, trions display three steps in σ reflecting the reduced tri-partite periodicity of the current. For CSF states, we find a characteristic TOF with decreased density in the centre of the interference pattern. By analysing, the different colour contributions to the TOF, we

deduced that the images arise as superpositions of the hole corresponding to the delocalized weakly coupled species and the smeared peak corresponding to the bound state of the paired particles. Such bound states are found to be characterized in TOF by just two steps in σ (reflecting the particle pairing) (Fig. 4).

Conclusions

In this paper, we studied the bound states of attracting three-component fermions through the frequency of the persistent current
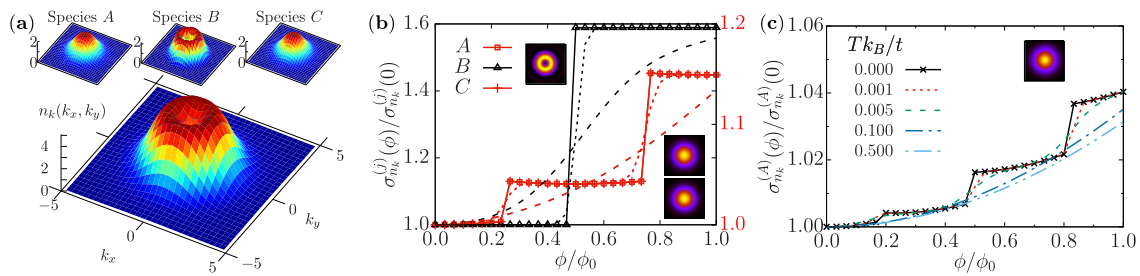
Fig. 4 Time-of-Flight (TOF) expansion for colour superfluids (CSFs) and trions. a TOF expansion of the CSF configuration. Main (top) panel displays the TOF expansion, $n(k)$, in arbitrary units for all (each) colours. Interactions are set to $|U_{AB}|/t = |U_{BC}|/t = 0.01$ and $|U_{AC}|/t = 5$. **b, c** Variance of width of the TOF expansion, $\sigma_{n_k}(\phi)$, against the effective magnetic flux ϕ. **b** shows the CSF configuration and $|U_{AB}|/t = |U_{BC}|/t = 0.01$ and $|U_{AC}|/t = 5$ for $Tk_B/t = \{0, 0.01, 0.1\}$, solid, dotted and dashed lines respectively. The secondary y-axis (red ticks) corresponds to the variance of the paired species (red lines). **c** shows the trionic configuration at $|U|/t = 5$ for different Tk_B/t. Insets next to the curves in **b** show the momentum distribution $n_k(k_x, k_y)$ at $\phi = 1$ of each component while in **c** we only show one colour due to SU(3) symmetry. Note that a colour bar was omitted from **a** as the values of the momentum distribution are displayed on the z-axis. Furthermore, the insets in **b, c** convey a qualitative description of the momentum distribution, with yellow (black) indicating a maximum (minimum) in the momentum distribution. The presented results are done for $N_p = 3$, $L = 10$ using exact diagonalization.

$I(\phi)$ both at zero and finite temperature. To this end, we apply a combination of Bethe ansatz and numerical methods that, especially for the finite temperature results, are among the very few non-perturbative approaches that can be applied to our system. Our analysis hinges on the fact that the effective flux quantum, defined by the frequency of $I(\phi)$ provides information on the nature of the particles involved in $I(\phi)$[4,37,38,43]. For our specific system of attractive SU(3) fermions, such a frequency indicates that three-colour bound states are formed, irrespective of the number of particles. This $N = 3$ case is the general feature we find for SU(N) attracting fermions whose bound states are formed by N particles; in contrast to repulsive fermions and attractive bosons in which the frequency is fixed by the number of particles. Our analysis can clearly distinguish between trions and CSFs: the first are characterized by the persistent currents of the three species displaying a periodicity that is increasingly reduced by interaction until reaching 1/3 of the original periodicity (for large interaction); CSFs, instead, result in persistent currents having two different periodicities for the different species (Fig. 1).

Finite temperature T induces specific changes in the persistent current frequency. We analysed the interplay between interaction and thermal fluctuations quantitatively and obtained specific laws describing it. For mild interactions, the frequency of $I(\phi)$ changes as result of the population of the scattering states. Indeed, we observe that the phenomenon occurs as a crossover from a colourless bound state to coloured multiplets, governed by the ratio U/T without an explicit SU(3) breaking (Figs. 2 and Fig. 3a). Although specific non-perturbative effects near the QCD transition are missed by our analogue system (such as string breaking and colour charge screening), the bound states' deconfinement in this regime displays similarities with the Quark-Gluon plasma formation at large T and small baryonic density[57]. Moreover, the introduction of a chemical potential, μ, could permit us to study of the "critical line" in the T-μ plane, in analogy with QCD at finite temperature and density, related with relativistic, but lower energy, heavy ion collisions and with the equation of state in the neutron stars core[58,59]. However this aspect requires a dedicated forthcoming analysis. For stronger attraction, the system defines a gas of bound states separated from the scattering states by a finite energy gap. In this regime, a 'single particle' thermal persistent current arises from the combination of the frequencies characterizing the different energy levels in the bound state sub-band (Fig. 3c). In the cross-over region between the scattering-states dominated and the gas of bound states, the change of the frequency of $I(\phi)$ takes place with an identical functional dependence on U and T (Fig. 3). For increasing interaction, the bound states' sub-band gets tighter and, therefore the temperature is increasingly relevant to wash out the fractionalization of the persistent current's periodicity.

The suggested implementation of our work is provided by cold atoms. Thus, we studied the time-of-flight images of the system obtained by releasing the cold atoms from the trap (Fig. 4). Additionally, we point out that recent advancements in the platform of programmable tweezers have paved the way to experimentally realize fermionic ring lattices[60]. This way, we believe that most of the presented results can be tested experimentally within the current cold atoms quantum technology infrastructure.

To conclude, we briefly comment on the phenomenon of three-body losses. In principle, these losses can be due to the presence of Efimov states[61]. However, we note that, unless specifically tuned, Efimov states occur as excited states[62], and as such they are not expected to impact the nature of the ground-state. Although, the formation of a stable three-component Fermi gas has been experimentally realized[63], experimental studies of three-body losses in one-dimensional SU(3) fermions are still lacking. In the case of spinless and SU(2) fermions, three-body losses are suppressed on account of the Pauli exclusion principle. However, the exclusion statistics of SU(3) fermions could allow the possibility of three-body recombination. In the case of bosonic systems, this phenomenon is suppressed in one-dimensional systems and thus by employing a similar logic, we expect a similar behaviour occurs in our system[61,62,64]. Whilst there is not a general consensus on the explanation, the theoretical analysis on bosonic systems indicates that the characteristic increase in the 1D scattering length[65] may result in a lower probability of forming resonant bound states[66].

Methods

The method employed utilizes a combination of numerical methods such as exact diagonalization and DMRG[67,68], as well as Bethe ansatz results whenever possible, in order to identify and characterize the bound states of SU(3) fermions, for systems with an equal number of particles N_p per colour. In particular, the zero temperature properties are addressed through DMRG; finite temperature results are obtained through exact diagonalization. As was already pointed out, the model is Bethe ansatz integrable in the case of certain parameters and filling fractions. Such constraints make the finite temperature analysis out of reach of Bethe ansatz.

Data availability

The data supporting the findings in this study are available from the corresponding author upon reasonable request.

Code availability

The codes utilized in this study are available from the corresponding author upon reasonable request.

References

1. Strecker, K. E., Partridge, G. B., Truscott, A. G. & Hulet, R. G. Formation and propagation of matter-wave soliton trains. *Nature* **417**, 150–153 (2002).
2. Kanamoto, R., Saito, H. & Ueda, M. Symmetry breaking and enhanced condensate fraction in a matter-wave bright soliton. *Phys. Rev. Lett.* **94**, 090404 (2005).
3. Calabrese, P. & Caux, J.-S. Dynamics of the attractive 1D Bose gas: analytical treatment from integrability. *J. Stat. Mech. Theory Exp.* **2007**, P08032–P08032 (2007).
4. Naldesi, P. et al. Rise and fall of a bright soliton in an optical lattice. *Phys. Rev. Lett.* **122**, 053001 (2019).
5. Leggett, A. J. et al. *Quantum Liquids: Bose Condensation and Cooper Pairing in Condensed-Matter Systems* (Oxford University Press, 2006).
6. Scazza, F. et al. Observation of two-orbital spin-exchange interactions with ultracold SU(N)-symmetric fermions. *Nat. Phys.* **10**, 779–784 (2014).
7. Hofrichter, C. et al. Direct probing of the Mott crossover in the SU(N) Fermi-Hubbard model. *Phys. Rev. X* **6**, 021030 (2016).
8. Gorshkov, A. V. et al. Two-orbital SU(N) magnetism with ultracold alkaline-earth atoms. *Nat. Phys.* **6**, 289–295 (2010).
9. Cazalilla, M. A. & Rey, A. M. Ultracold Fermi gases with emergent SU(N) symmetry. *Rep. Prog. Phys.* **77**, 124401 (2014).
10. Capponi, S., Lecheminant, P. & Totsuka, K. Phases of one-dimensional SU(N) cold atomic Fermi gases-from molecular Luttinger liquids to topological phases. *Ann. Phys.* **367**, 50–95 (2016).
11. Sonderhouse, L. et al. Thermodynamics of a deeply degenerate SU(N)-symmetric Fermi gas. *Nat. Phys.* **16**, 1216–1221 (2020).
12. Greensite, J. *An Introduction to the Confinement Problem* (Springer Berlin Heidelberg, 2011).
13. Cherng, R. W., Refael, G. & Demler, E. Superfluidity and magnetism in multicomponent ultracold fermions. *Phys. Rev. Lett.* **99**, 130406 (2007).
14. Rapp, A., Zaránd, G., Honerkamp, C. & Hofstetter, W. Color superfluidity and "Baryon" formation in ultracold fermions. *Phys. Rev. Lett.* **98**, 160405 (2007).
15. Klingschat, G. & Honerkamp, C. Exact diagonalization study of trionic crossover and trion liquid in the attractive three-component hubbard model. *Phys. Rev. B* **82**, 094521 (2010).
16. Baym, G. BCS from nuclei and neutron stars to quark matter and cold atoms. *Int. J. Mod. Phys. B* **24**, 3968–3982 (2010).
17. Rico, E. et al. SO (3) "nuclear physics" with ultracold gases. *Ann. Phys.* **393**, 466–483 (2018).
18. Banerjee, D. et al. Atomic quantum simulation of dynamical gauge fields coupled to fermionic matter: from string breaking to evolution after a quench. *Phys. Rev. Lett.* **109**, 175302 (2012).
19. Tajima, H., Tsutsui, S., Doi, T. M. & Iida, K. Cooper triples in attractive three-component fermions: implication for hadron-quark crossover. *Phys. Rev. Res.* **4**, L012021 (2021).
20. Dalmonte, M. & Montangero, S. Lattice gauge theory simulations in the quantum information era. *Contemp. Phys.* **57**, 388–412 (2016).
21. Honerkamp, C. & Hofstetter, W. BCS pairing in Fermi systems with N different hyperfine states. *Phys. Rev. B* **70**, 094521 (2004).
22. Catelani, G. & Yuzbashyan, E. A. Phase diagram, extended domain walls, and soft collective modes in a three-component fermionic superfluid. *Phys. Rev. A* **78**, 033615 (2008).
23. Capponi, S. et al. Molecular superfluid phase in systems of one-dimensional multicomponent fermionic cold atoms. *Phys. Rev. A* **77**, 013624 (2008).
24. Batchelor, M. T., Foerster, A., Guan, X.-W. & Kuhn, C. C. N. Exactly solvable models and ultracold Fermi gases. *J. Stat. Mech. Theory Exp.* **2010**, P12014 (2010).
25. Kuhn, C. C. N. & Foerster, A. Phase diagrams of three-component attractive ultracold fermions in one dimension. *N. J. Phys.* **14**, 013008 (2012).
26. Pohlmann, J., Privitera, A., Titvinidze, I. & Hofstetter, W. Trion and dimer formation in three-color fermions. *Phys. Rev. A* **87**, 023617 (2013).
27. Guan, X.-W., Batchelor, M. T. & Lee, C. Fermi gases in one dimension: from Bethe ansatz to experiments. *Rev. Mod. Phys.* **85**, 1633–1691 (2013).
28. Imry, Y. *Introduction to Mesoscopic Physics* (Oxford University Press, 2002).
29. Amico, L. et al. Roadmap on atomtronics: state of the art and perspective. *AVS Quant. Sci.* **3**, 039201 (2021).
30. Amico, L. et al. Colloquium: Atomtronic circuits: from many-body physics to quantum technologies. *Rev. Mod. Phys.* **94**, 041001 (2022).
31. Ryu, C. et al. Observation of persistent flow of a Bose-Einstein condensate in a toroidal trap. *Phys. Rev. Lett.* **99**, 260401 (2007).
32. Ramanathan, A. et al. Superflow in a toroidal Bose-Einstein condensate: an atom circuit with a tunable weak link. *Phys. Rev. Lett.* **106**, 130401 (2011).
33. Pandey, S. et al. Hypersonic Bose–Einstein condensates in accelerator rings. *Nature* **570**, 205–209 (2019).
34. Ögren, M., Drougakis, G., Vasilakis, G., von Klitzing, W. & Kavoulakis, G. M. Stationary states of Bose–Einstein condensed atoms rotating in an asymmetric ring potential. *J. Phys. B At., Mol. Optical Phys.* **54**, 145303 (2021).
35. Cai, Y., Allman, D. G., Sabharwal, P. & Wright, K. C. Persistent currents in rings of ultracold fermionic atoms. *Phys. Rev. Lett.* **128**, 150401 (2022).
36. Del Pace, G. et al. Imprinting persistent currents in tunable fermionic rings. *Phys. Rev. X* **12**, 041037 (2022).
37. Leggett, A. J. *Dephasing and Non-Dephasing Collisions in Nanostructures* 297–311 (Springer US, 1991).
38. Byers, N. & Yang, C. N. Theoretical considerations concerning quantized magnetic flux in superconducting cylinders. *Phys. Rev. Lett.* **7**, 46–49 (1961).
39. Onsager, L. Magnetic flux through a superconducting ring. *Phys. Rev. Lett.* **7**, 50–50 (1961).
40. Polo, J., Naldesi, P., Minguzzi, A. & Amico, L. Exact results for persistent currents of two bosons in a ring lattice. *Phys. Rev. A* **101**, 043418 (2020).
41. Naldesi, P. et al. Enhancing sensitivity to rotations with quantum solitonic currents. *SciPost Phys.* **12**, 138 (2022).
42. Polo, J., Naldesi, P., Minguzzi, A. & Amico, L. The quantum solitons atomtronic interference device. *Quant. Sci. Technol.* **7**, 015015 (2021).
43. Chetcuti, W. J., Haug, T., Kwek, L.-C. & Amico, L. Persistent current of SU(N) fermions. *SciPost Phys.* **12**, 33 (2022).
44. Richaud, A., Ferraretto, M. & Capone, M. Interaction-resistant metals in multicomponent Fermi systems. *Phys. Rev. B* **103**, 205132 (2021).
45. Beattie, S., Moulder, S., Fletcher, R. J. & Hadzibabic, Z. Persistent currents in spinor condensates. *Phys. Rev. Lett.* **110**, 025301 (2013).
46. Lewenstein, M., Sanpera, A. & Ahufinger, V. *Ultracold Atoms in Optical Lattices: Simulating Quantum Many-Body Systems* (Oxford University Press, 2012).
47. Sutherland, B. Further results for the many-body problem in one dimension. *Phys. Rev. Lett.* **20**, 98–100 (1968).
48. Takahashi, M. Many-body problem of attractive fermions with arbitrary spin in one dimension. *Prog. Theor. Phys.* **44**, 899–904 (1970).
49. Takahashi, M. *Thermodynamics of One-Dimensional Solvable Models* (Cambridge University Press, 1999).
50. Sutherland, B. Model for a multicomponent quantum system. *Phys. Rev. B* **12**, 3795–3805 (1975).
51. Pecci, G., Naldesi, P., Amico, L. & Minguzzi, A. Probing the BCS-BEC crossover with persistent currents. *Phys. Rev. Res.* **3**, L032064 (2021).
52. Amico, L., Osterloh, A. & Cataliotti, F. Quantum many particle systems in ring-shaped optical lattices. *Phys. Rev. Lett.* **95**, 063201 (2005).
53. Yu, N. & Fowler, M. Persistent current of a Hubbard ring threaded with a magnetic flux. *Phys. Rev. B* **45**, 11795–11804 (1992).
54. Pâţu, O. I. & Averin, D. V. Temperature-dependent periodicity of the persistent current in strongly interacting systems. *Phys. Rev. Lett.* **128**, 096801 (2022).
55. Pecci, G., Naldesi, P., Minguzzi, A. & Amico, L. Single-particle versus many-body phase coherence in an interacting Fermi gas. *Quant. Sci. Technol.* **8**, 01LT03 (2022).
56. Chetcuti, W. J., Osterloh, A., Amico, L. & Polo, J. Interference dynamics of matter-waves of SU(N) fermions. Preprint at https://arxiv.org/abs/2206.02807 (2022).
57. Satz, H. Probing the states of matter in QCD. *Int. J. Mod. Phys. A* **28**, 1330043 (2013).
58. Andronic, A., Braun-Munzinger, P., Redlich, K. & Stachel, J. Decoding the phase structure of QCD via particle production at high energy. *Nature* **561**, 321–330 (2018).
59. Annala, E., Gorda, T., Kurkela, A., Nättilä, J. & Vuorinen, A. Evidence for quark-matter cores in massive neutron stars. *Nat. Phys.* **16**, 907–910 (2020).
60. Yan, Z. Z. et al. Two-dimensional programmable tweezer arrays of fermions. *Phys. Rev. Lett.* **129**, 123201 (2022).
61. Naidon, P. & Endo, S. Efimov physics: a review. *Rep. Prog. Phys.* **80**, 056001 (2017).
62. Williams, J. et al. Evidence for an excited-state Efimov trimer in a three-component Fermi gas. *Phys. Rev. Lett.* **103**, 130404 (2009).
63. Ottenstein, T. B., Lompe, T., Kohnen, M., Wenz, A. N. & Jochim, S. Collisional stability of a three-component degenerate Fermi gas. *Phys. Rev. Lett.* **101**, 203202 (2008).
64. Chen, X.-Y. et al. Suppression of unitary three-body loss in a degenerate Bose-Fermi mixture. *Phys. Rev. Lett.* **128**, 153401 (2022).
65. Olshanii, M. Atomic scattering in the presence of an external confinement and a gas of impenetrable bosons. *Phys. Rev. Lett.* **81**, 938 (1998).
66. Mehta, N. P., Esry, B. & Greene, C. H. Three-body recombination in one dimension. *Phys. Rev. A* **76**, 022711 (2007).
67. White, S. R. Density matrix formulation for quantum renormalization groups. *Phys. Rev. Lett.* **69**, 2863–2866 (1992).

68. Fishman, M., White, S. R. & Stoudenmire, E. M. The ITensor software library for tensor network calculations. SciPost Physics Codebases 4. https://scipost.org/10.21468/SciPostPhysCodeb.4 (2022).

Author contributions
L.A. conceived the idea of the project. W.J.C. and J.P. generated the data and the figures. W.J.C., J.P., A.O., P.C. and L.A. contributed equally to the scientific discussion and writing of the manuscript.

Competing interests
The authors declare no competing interests.

Additional information
Supplementary information The online version contains supplementary material available at https://doi.org/10.1038/s42005-023-01256-3.

Correspondence and requests for materials should be addressed to Wayne J. Chetcuti.

Peer review information *Communications Physics* thanks the anonymous reviewers for their contribution to the peer review of this work. A peer review file is available.

Reprints and permission information is available at http://www.nature.com/reprints

Publisher's note Springer Nature remains neutral with regard to jurisdictional claims in published maps and institutional affiliations.